DETERMINING THE TRANSVERSE DIMENSIONS OF FIBERS IN WOOD USING CONFOCAL MICROSCOPY

Ho Fan Jang
Scientist

Rajinder S. Seth
Principal Scientist

Cheng Bao Wu
Technical Specialist

and

Ben K. Chan
Technical Specialist
Pulp and Paper Research Institute of Canada
3800 Wesbrook Mall
Vancouver, BC
Canada V6S 2L9

(Received August 2004)

ABSTRACT

We describe a technique for determining the transverse dimensions of individual fibers in wood using confocal laser scanning microscopy and image analysis. Optical sectioning of confocal microscopy produces high-quality cross-sectional images of large wood samples, thus eliminating the need for traditional mechanical sectioning and its inherent limitations. The relationships between fiber transverse dimensions of wood and kraft pulp fibers, in terms of their means and distributions, are now established. Measuring fibers in wood also allows us now to evaluate properties of early- and latewood separately, and to better understand the origin of heterogeneity. Relative wood density obtained from a wood section correlates strongly to the ratio of fiber wall thickness to perimeter, which is an important parameter for fiber transverse collapse. This direct and accurate method has the potential for automation, thus allowing a rapid assessment of wood quality for papermaking.

Keywords: Confocal microscopy, image analysis, cell-wall thickness, fiber dimensions, wood density, wood structure.

INTRODUCTION

The morphological properties of pulp fibers—particularly their transverse dimensions such as wall cross-sectional area, perimeter, and thickness—influence how fibers respond to processing and strongly affect the properties of end products (Seth 1990). However, fiber transverse dimensions are difficult to measure. Recently, we have developed procedures for obtaining cross-sectional images of wood pulp fibers using the optical sectioning ability of confocal laser scanning microscopy (CLSM) (Jang et al. 1991; 1992). Combining this with image analysis, we are able to accurately obtain fiber transverse dimensions and their distributions (Seth et al. 1997). However, these procedures are time-consuming, requiring manually locating and aligning individual fibers before their cross-sectional images can be generated.

The fiber transverse dimensions in wood and pulp made from that wood are shown to be related through pulp yield (Scallan and Green

Dr. Rajinder S. Seth, one of the co-authors of this article, regrettably passed away on July 31, 2005, after a courageous battle with a long illness.

Wood and Fiber Science, 37(4), 2005, pp. 615–628

1975). Fiber transverse dimensions can be obtained directly from wood cross-sections, each of them containing numerous fiber cross-sections. The traditional mechanical sectioning methods of preparing cross-sections for microscopic examination are tedious, and are prone to misinterpretation because of the limited sample size and the artifacts of specimen preparation and imaging. SilviScan (Evans et al. 1995), a newly developed system for rapid characterization of wood and fiber quality based on X-ray densitometry and image analysis, provides values for the mean fiber coarseness in a measurement zone. This indirect technique is fast, but in general has narrower applicability than direct techniques for individual fiber measurements.

In our search for direct, rapid, and accurate methods to obtain individual fiber transverse dimensions, we examined the feasibility of making such measurements directly on wood using the unique ability of confocal microscopy to produce optical sections, thus avoiding the inherent limitations of mechanical sectioning. Recent work has shown that optical sectioning produces more accurate images of wood cells compared to conventional microscopy using thick sections for imaging by transmitted light microscopy (Donaldson and Lausberg 1998). The main objective of our work was to demonstrate that fiber transverse dimensions can be determined rapidly and accurately, without pulping, by making measurements directly on wood using confocal microscopy and image analysis.

In this report, we first show that high-quality cross-sectional images of large wood samples can be generated easily by optical sectioning of CLSM. These images are then analyzed for individual fiber transverse dimensions, such as cross-sectional area, perimeter, and wall thickness, and for the relative wood density. These results were compared with measurements obtained from kraft pulp fibers taken from the same wood sample. Fiber transverse dimensions in earlywood and latewood, and their relationships to wood density are shown. Implications of latewood content for heterogeneity, and of wood density for fiber collapse are discussed.

EXPERIMENTAL

Sample preparation

Wood samples in the form of small blocks (~1.5 × 2 cm^2 in area) were taken from about 2.5-cm-thick discs from four different western hemlock trees; kraft pulps made from the adjacent wood samples from each tree were available from a previous investigation (King et al. 1998). These trees were plantation-grown, 13 years old; and the sample discs were taken at breast height. All samples from each tree were taken from the three outermost annual rings (10 to 13) as shown in Fig. 1. The pulps were made to a Kappa number of about 30 (corresponding to a lignin content of about 5%). The procedure for preparing unbleached kraft pulps from small wood samples is described elsewhere (Gee and Hatton 1991). The results for wood density and pulp yield are given in Table 1.

Kraft pulp and wood-block samples were prepared for confocal imaging. The procedures for dyeing pulp fibers with a fluorochrome, and preparing them for optical sectioning with confocal microscopy have been described previously (Jang et al. 1992). Wood samples did not require dyeing because of the inherent strong autofluorescence of lignin. They were prepared for optical sectioning as follows. Each sample was first extracted with acetone for 24 h to remove wood resins, and then reconditioned at room temperature. Since the confocal microscope has a limited depth of penetration, a smooth sample surface was required for high quality imaging. A

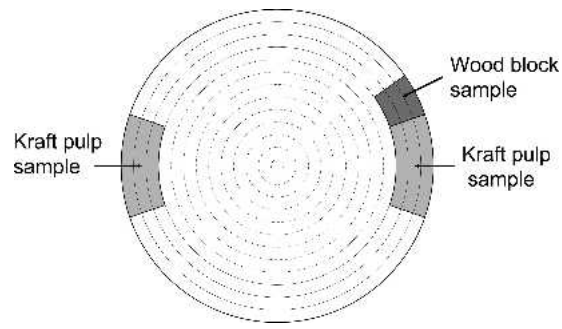

FIG. 1. Schematic of sampling wood for pulping and for microscopical evaluation.

TABLE 1. *Wood density and pulp yield of samples.*

Sample number	Wood‡ density, kg/m^3	Pulp yield, %
1	360	44.4
2	530	44.7
3	482	43.5
4	452	44.5

‡ Wood density was measured as oven-dried mass per unit wet-wood (green) volume.

sample preparation technique similar to that developed by Williams and Drummond (2000) for cross-sectioning paper samples was used. The technique involves embedding the samples in a resin, curing the resin, polishing the surface, and etching away a thin layer of the embedded resin from the viewing surface. The wood samples were then mounted in immersion oil under cover slips. We chose an embedding medium with a refractive index close to that of the wood, as this helped in obtaining higher quality confocal images.

Confocal microscopy

A Bio-Rad MRC-600 confocal laser scanning system, attached to a Nikon microscope operated in epifluoresence mode, was used for obtaining fiber cross-sectional images both from pulp and wood. Imaging was done using a 60× oil-immersion Plan-Apochromatic objective lens with a numerical aperture of 1.4. The pinhole was adjusted to achieve the best possible longitudinal resolution while maintaining sufficient signal intensity. The procedure for generating and analyzing images from single pulp fibers has been reported earlier (Jang et al. 1992; Chan et al. 1998). A typical fluorescence cross-sectional image of wood obtained with CLSM is shown in Fig. 2. Over 50 such images were collected for each wood with sampling on a square grid pattern.

Analysis for wood cross-sectional images

Individual fiber transverse dimensions were obtained from wood cross-sections using an image analyzer (IBAS, Kontron Elektronik GmbH, Germany). The image analysis steps, which were adapted from those of Travis et al. (1996), are illustrated in Fig. 3. The wood cross-sectional image shown in Fig. 2 is a gray-level image. The first step in image analysis was to separate, through segmentation, the fiber wall material (shown in white) from the lumen or background (shown in black) (Fig. 3a). A more complex edge-detection routine was not required because the lateral resolution of the images was high. The second step was to approximate the positions of the fiber-fiber boundaries. To achieve this, a skeletonization routine could have been applied to the binary fiber wall image in Fig. 3a. However, skeletonization is a mathematically intense operation that takes a long time, especially for thick-walled fibers. Instead, a distance transform routine was applied to the binary fiber wall image in Fig. 3a. In the distance transform image (Fig. 3b), the gray value of each pixel corresponds to the distance from that pixel to the nearest fiber wall–lumen boundary. The gray values reach their maxima at the midpoints of the fiber walls. The fiber-fiber boundaries were then approximated by segmenting the distance transform image into a binary image, and then skeletonizing the binary image into a single-pixel wide fiber wall boundary image (Fig. 3c). In the procedure published by Travis et al. (1996), a "watershed" algorithm was used to identify local maxima in the distance transform image (Chan et al. 1998). However, this routine was not available on the IBAS. Overlaying the fiber wall boundary image on the original wood cross-sectional image shows that the approximated fiber boundaries overlap the middle la-

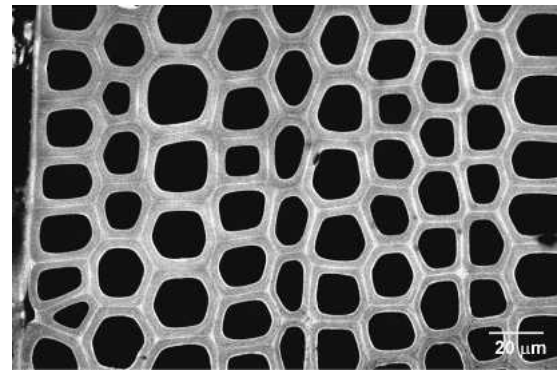

FIG. 2. Fluorescence cross-sectional image of softwood obtained with CLSM.

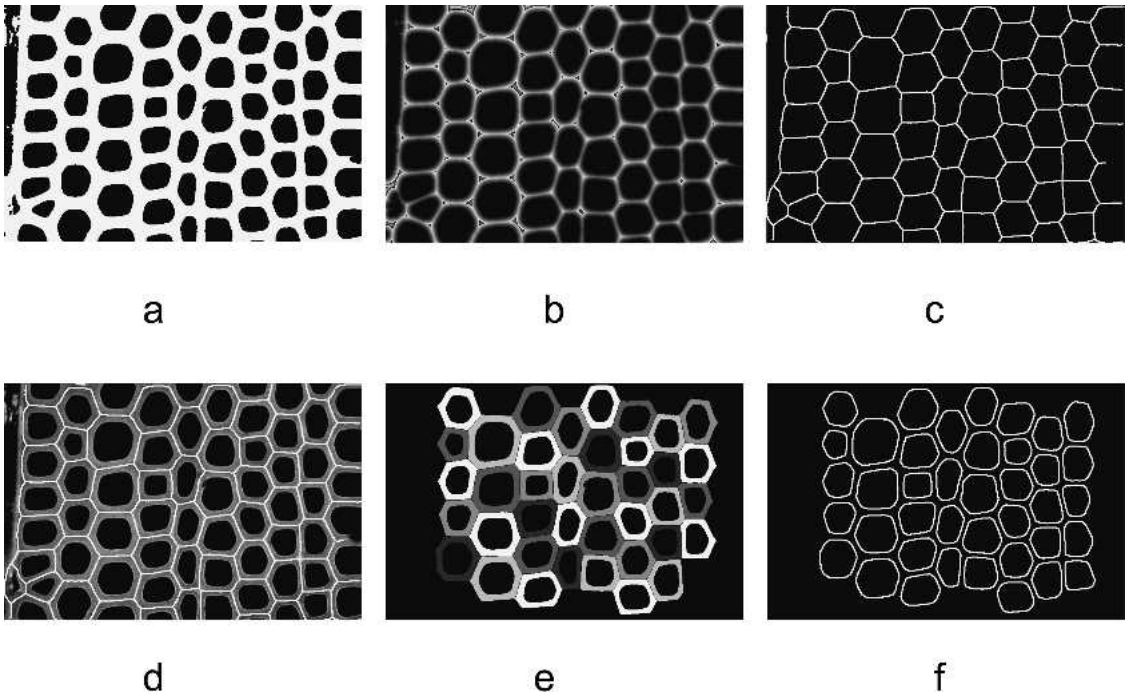

FIG. 3. Image analysis steps for a wood cross-sectional image: (a) segmentation, (b) distance transform, (c) skeletonization, (d) fiber wall boundary, (e) fiber separation, and (f) fiber center-line perimeter.

mella (Fig. 3d). By masking the binary fiber wall image (Fig. 3a) with the fiber wall boundary image (Fig. 3c), individual fibers can be separated and labeled as shown in Fig. 3e. Fiber transverse dimensions, such as fiber wall cross-sectional area, lumen area, and outer fiber, and lumen perimeters can then be measured from the image. Since the fiber wall boundary (one pixel wide) occupies a finite area, the fiber wall cross-sectional area was corrected by adding half of the area of its boundary.

A skeletonization routine was then applied to the binary image (Fig. 3e) to generate fiber center-line perimeters (Fig. 3f). Fiber wall thickness could then be calculated by dividing the fiber wall cross-sectional area by the center-line perimeter.

RESULTS AND DISCUSSION

Wood vs. pulp fiber transverse dimensions

We compared the following fiber transverse dimensions: wall cross-sectional area A, center-line perimeter P, outer perimeter OP, lumen perimeter LP, and the wall thickness T calculated as A/P. Figure 4 shows plots of mean fiber transverse dimensions for the four wood samples plotted against those obtained for the corresponding pulps. The least-square fits through the data are also shown. The slope of the line in Fig. 4a is 0.45 ± 0.01. This implies that the mean fiber wall cross-sectional area of pulp fibers was about 45% of that of the fibers in wood. This agrees with the pulp yields that ranged from 44 to 45% as shown in Table 1. Note that the length of wood fibers also shrinks about 4% upon pulping (Scallan and Green 1975); therefore, fiber cross-sectional area should be expected to shrink to only about 47% instead of the actual 45% of the original at 45% yield. The 2% difference could be explained in terms of the different densities of the various chemical constituents of the fiber. Lignin and hemicelluloses have somewhat lower densities than cellulose (by a few percent), and thus the removal of lignin and hemicellu-

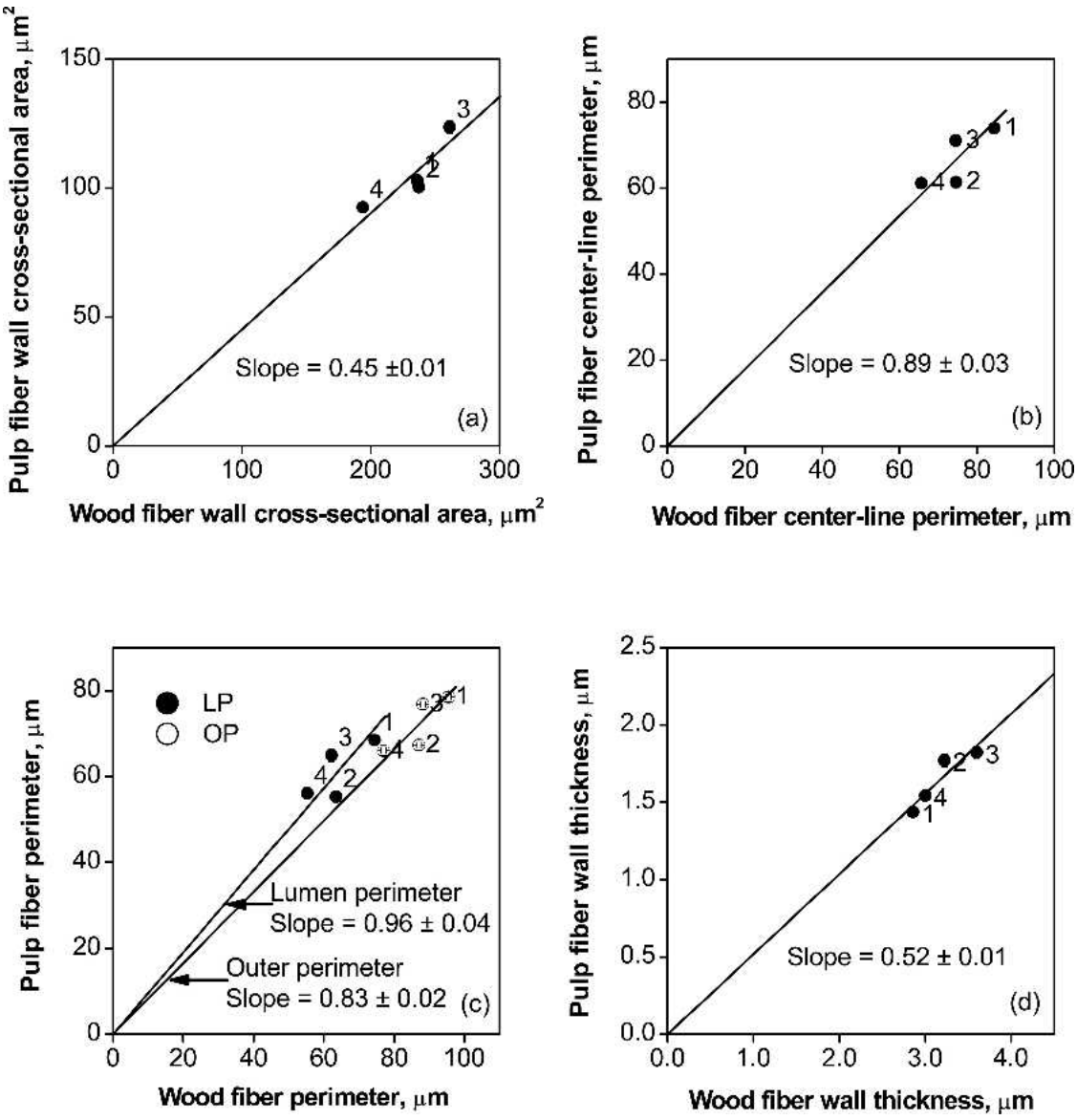

FIG. 4. Wood vs. pulp fiber transverse dimensions.

loses during kraft pulping may result in a greater percent reduction in cross-sectional area than in weight.

Figures 4b and 4c show that after pulping, the fiber center-line perimeter shrank to 89 ± 3% of the original in the wood, while the lumen and outer perimeters shrank to 96 ± 4% and 83 ± 2%, respectively. The reduction in fiber wall thickness, which shrank to 52 ± 1% of the original in the wood, was much greater than those in the fiber perimeters (Fig. 4d). These observations are consistent with those of Scallan and Green (1975), and agree with a fiber wall structure that is based on layers of cellulose fibrils embedded in a lignin-hemicellulose matrix. This is further discussed in Appendix A.

Figure 5 shows the empirical distribution functions for the transverse dimensions *A*, *P*, *LP*,

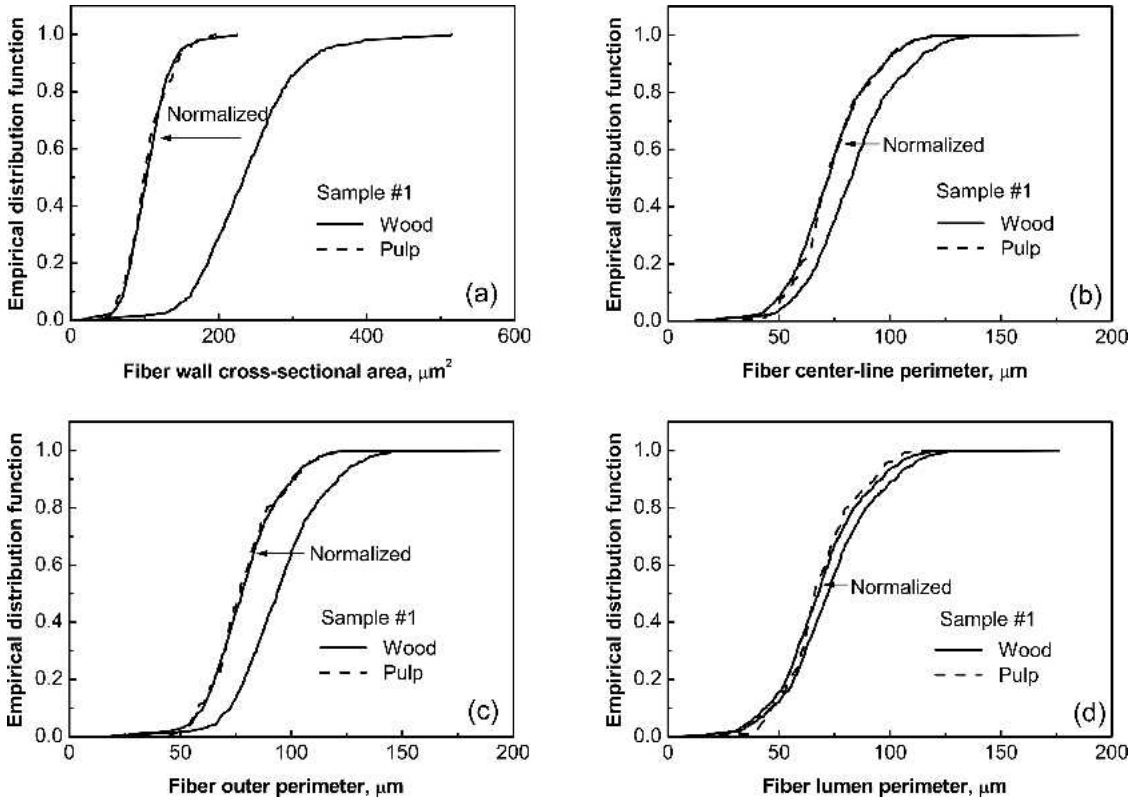

FIG. 5. Empirical distribution functions for *A*, *P*, *LP*, and *OP* of wood and pulp fibers. The distributions for wood data were normalized to have common means with the pulp data for comparison. The K-S tests show high significance levels for the normalized distributions of wood and pulp fiber properties.

and *OP* for wood and pulp fibers of sample No. 1. An empirical distribution function of a data set is a function that describes the fraction of the data points that are smaller than a given value. In order to compare the data directly, the wood data were normalized to the pulp data with a common mean. The Kolmogorov-Simirnov (K-S) test was used to determine the difference between the normalized distributions of wood and pulp data. The K-S test determines the probability that the two data sets are from the same population (Sprent 1993). The significance levels of the K-S test were found to be high (>35% significance level) for *A*, *P*, *LP*, and *OP* indicating that the distributions of these parameters in pulps were similar to those in the wood (Fig. 5) when the distributions were normalized to the same means.

However, when the K-S test was applied to the normalized fiber wall thickness distributions, the significance level was below 5% for all four samples. This indicated that the distributions were different, as illustrated in Fig. 6 for sample No. 1. The fiber wall thickness distributions for pulp were found to be broader and more variable than those for wood. Since wall thickness *T* is simply *A/P*, these findings were unexpected, but can be explained in terms of the pulp yield differences between early- and latewoods fibers (Appendix B).

Difference between early- and latewood fibers

Figure 7 shows a typical wood cross-sectional image at the earlywood–latewood ring boundary. Latewood usually has a higher proportion of fiber wall material per unit volume than the corresponding earlywood, and is therefore denser.

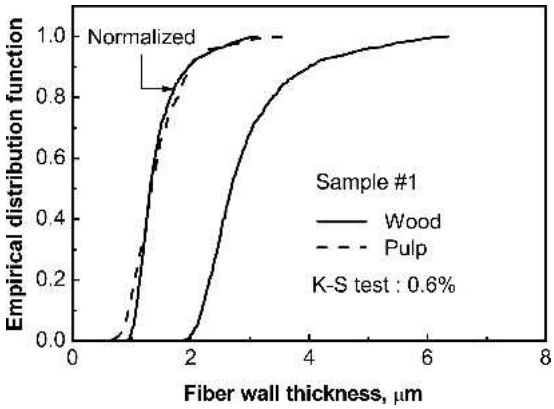

FIG. 6. Empirical distribution functions for *T* of wood and pulp fibers. The K-S test shows a low significance level for the normalized distributions.

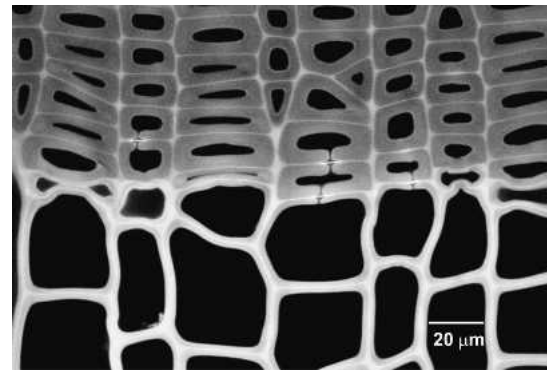

FIG. 7. Wood cross-section showing earlywood–latewood ring boundary.

As shown in Fig. 7, early- and latewood regions can be distinguished based on the area of fiber wall material per unit image area. Thus, we defined the relative density for each wood image as Eq. (1). Image area is simply the size of the image, and fiber wall area can be measured from the binary image shown in Fig. 3a. The relative density of the image shown in Fig. 7 was 0.495.

$$\text{Relative wood density} = \frac{\text{Fiber wall area}}{\text{Image area}} \qquad (1)$$

A relative density of 0.44 was chosen as the dividing line between early- and latewood. That is, fibers contained in the images having a density greater than 0.44 were classified as latewood. This division was arbitrary for these samples since the density change is continuous across the growth ring. Images containing the ring boundary such as that shown in Fig. 7 were not used.

The means and standard deviations of *A*, *P*, *T* and relative density for early- and latewoods of all four samples are given in Table 2. Note that the mean fiber wall cross-sectional areas for early- and latewood for samples Nos. 2, 3, and 4 are nearly similar, but the fiber wall thicknesses are quite different. As expected, earlywood fibers have larger perimeters and thinner walls than latewood fibers.

Figure 8 shows plots of *A*, *P*, and *T* of earlywood fibers against latewood fibers, including the linear regressions; the relative densities are also compared. Clearly, with the exception of *P*,

TABLE 2. *Mean and standard deviation (SD) of A, P, T, and relative density.*

Sample		Number of fibers (% of total)	A (SD), μm²	P (SD), μm	T (SD), μm	Relative wood density (SD)
#1	Earlywood	528 (73.6)	223 (55)	88.6 (20.5)	2.53 (0.34)	0.34 (0.06)
	Latewood	189 (26.4)	279 (82)	70.2 (14.8)	3.97 (0.87)	0.53 (0.08)
	Combined	717 (100)	236 (66)	84.5 (20.6)	2.86 (0.82)	0.37 (0.10)
#2	Earlywood	450 (54.6)	237 (71)	83.4 (21.4)	2.82 (0.27)	0.37 (0.04)
	Latewood	374 (45.4)	238 (71)	64.1 (15.2)	3.71 (0.67)	0.54 (0.08)
	Combined	824 (100)	238 (71)	74.6 (21.0)	3.22 (0.65)	0.43 (0.10)
#3	Earlywood	259 (28.2)	272 (69)	92.1 (21.4)	2.95 (0.34)	0.36 (0.04)
	Latewood	658 (71.8)	256 (68)	65.5 (13.7)	3.92 (0.70)	0.55 (0.08)
	Combined	917 (100)	261 (69)	74.5 (20.5)	3.60 (0.62)	0.47 (0.11)
#4	Earlywood	389 (33.4)	204 (52)	79.2 (15.9)	2.56 (0.25)	0.37 (0.04)
	Latewood	774 (66.6)	188 (54)	57.9 (12.8)	3.25 (0.63)	0.53 (0.08)
	Combined	1163 (100)	194 (54)	65.7 (17.4)	3.00 (0.64)	0.45 (0.10)

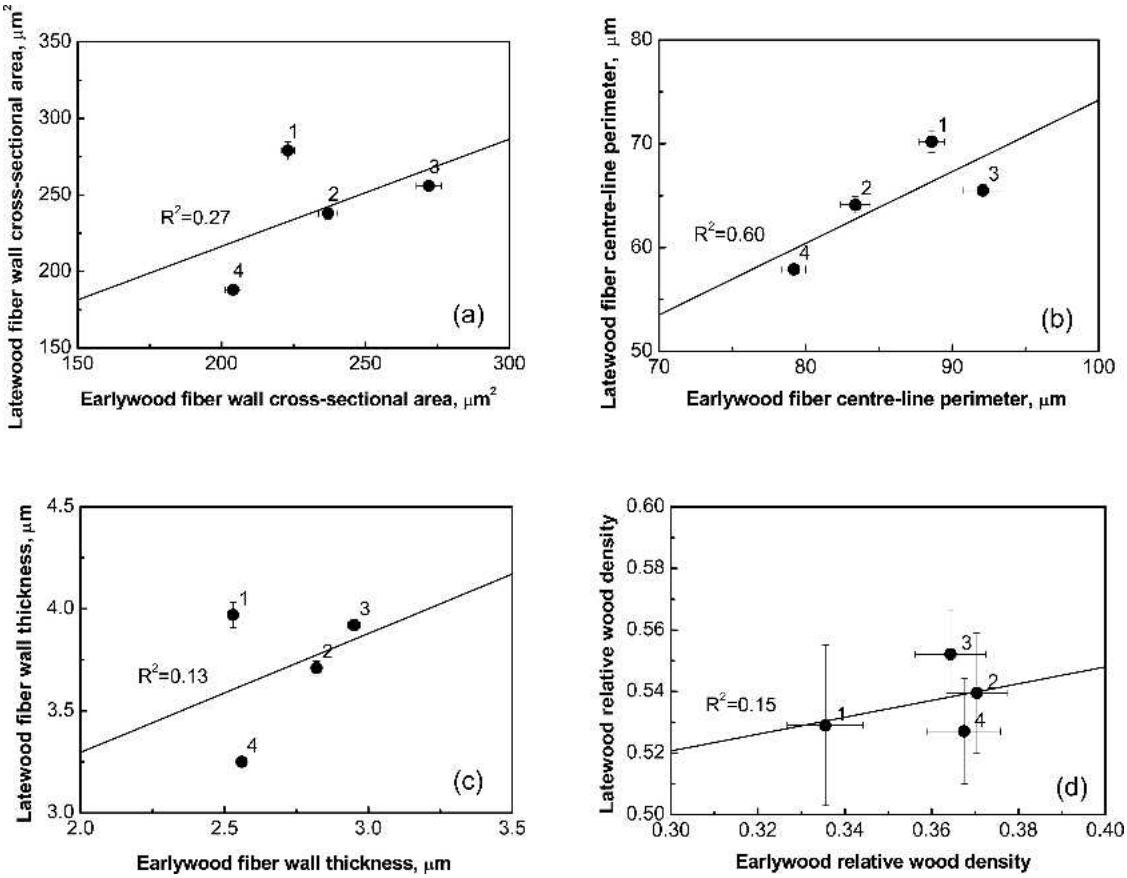

FIG. 8. Relationships between earlywood and latewood fiber transverse dimensions and wood density.

fiber properties, and the relative wood densities of early- and latewood are not well correlated for these four samples. It is not clear whether a correlation between early- and latewood fiber properties is to be expected.

Figure 9 shows, as an example, frequency distributions of *A*, *P*, and *T* for early- and latewood fibers in sample No. 1. The distributions were fitted with a three-parameter Weibull function (Seth et al. 1997). While the *A* and *P* distributions for both early- and latewood fibers were quite symmetric in shape, the distributions for *T* had some positive skewness, indicating greater heterogeneity in the populations; the distribution for the latewood being more skewed than that for the earlywood. The other three samples also showed similar patterns.

Our earlier work showed that species with coarser and thicker-walled fibers have more heterogeneous populations; the standard deviation is higher, when the mean is higher (Seth et al. 1997). Figure 10a and b show simple proportional relationships for standard deviations versus the means of *A*, and *P* for both early- and latewood fibers of these four samples. This implies that early- and latewood fibers have distributions of similar shape for *A* and *P* respectively. On the other hand, Fig. 10c shows different proportional relationships for wall thickness of early- and latewood fibers. This indicates that early- and latewood fibers have distributions of different shape for wall thickness, as evidenced in Fig. 9. Clearly, the thinner-walled earlywood fibers are much more homogeneous. Table 2 also shows different proportions of early- and latewood fibers in these wood samples. Since

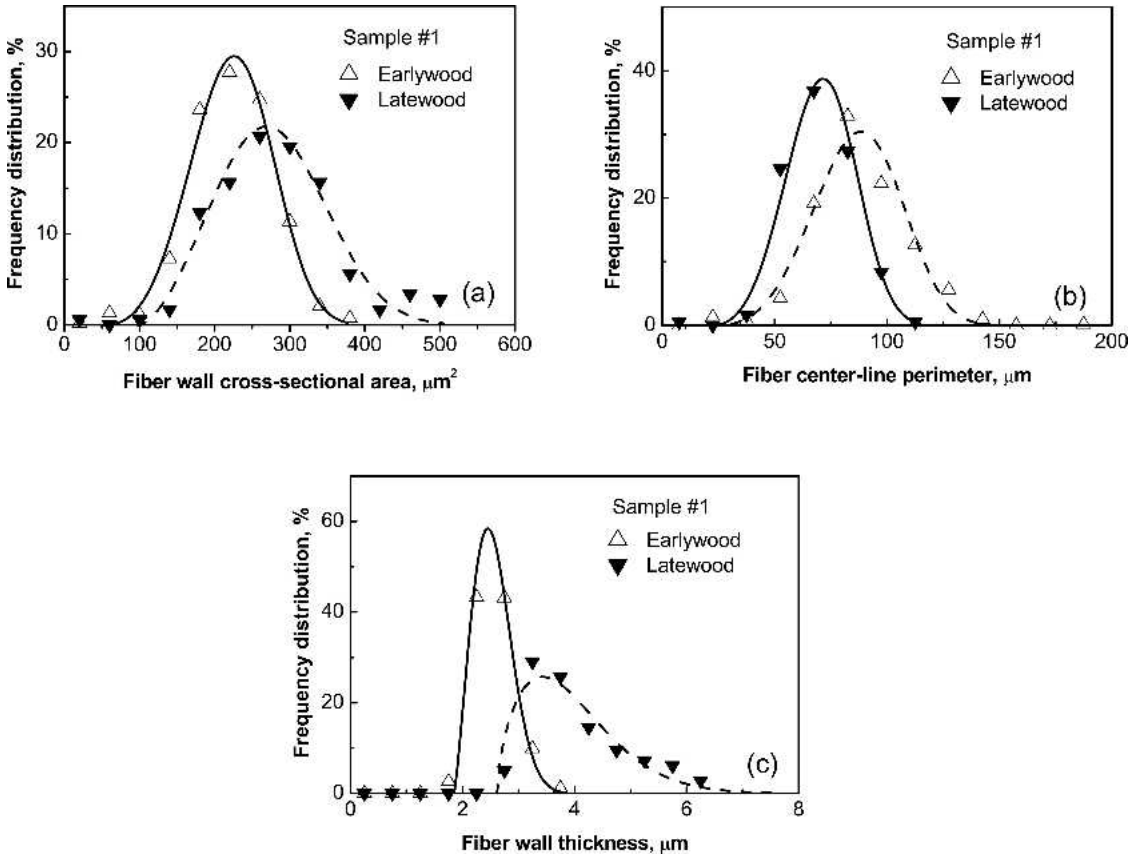

FIG. 9. Frequency distributions of *A*, *P*, and *T* for early- and latewood fibers in sample No. 1. The curves are fits with a three-parameter Weibull function (Seth et al. 1997).

fiber properties, especially wall thickness, are different in early- and latewood, the earlywood to latewood ratio plays a critical role in determining overall fiber transverse dimensions and heterogeneity of pulps. These factors are important for pulp quality.

Figure 11 shows how mean *A*, *P*, and *T* are interrelated for early- and latewood fibers in the four samples. For latewood fibers, *A*, *P*, and *T* are strongly correlated; a somewhat weaker correlation is evident for earlywood fibers. According to these results, fibers with a larger *A* will have a larger perimeter and thicker wall.

Figure 11b shows a simple proportional relationship between mean *T* and *P*, implying that *T/P* is similar for all four samples when early- and latewood fibers are considered separately. *T/P* is an important geometry factor that controls fiber collapse (Jang and Seth 1998; Jang 2001). However, the relationships among *A*, *P*, and *T* do not hold for the whole samples because the earlywood to latewood ratios vary between the different samples (Table 2). Fiber measurements on wood thus allow us to separately evaluate the fiber properties of early- and latewood, and to better understand the relationships among fiber transverse dimensions, and the origin of heterogeneity of fibers in wood.

Relationship between fiber transverse dimensions and wood density

Earlier, we defined the relative wood density as the ratio of fiber wall area to the image area. If all fibers in a wood sample had the same transverse dimensions, the relative wood density

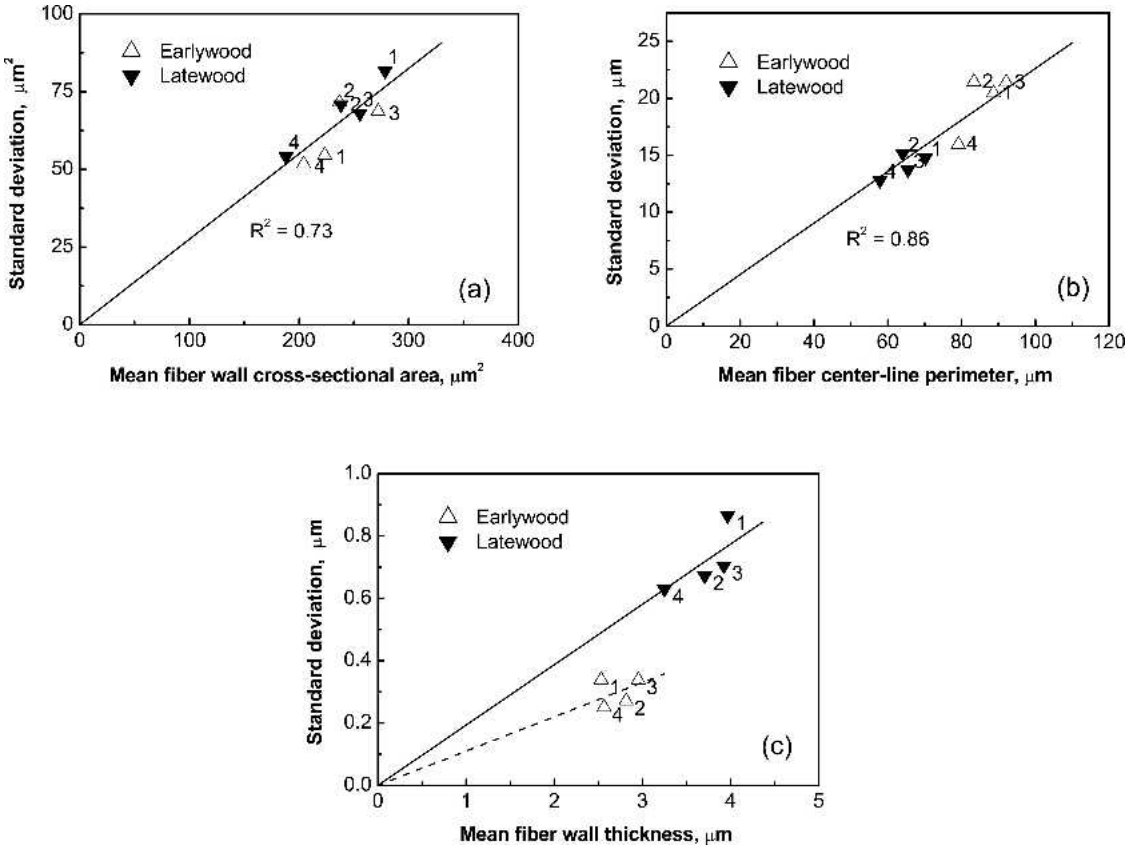

FIG. 10. Standard deviation versus mean for A, P, and T of early- and latewood fibers.

RWD would be equivalent to the relative density of a single fiber *RFD*. That is,

$$RWD = RFD = \frac{\text{Fiber wall area}}{\text{Total fiber area}} \qquad (2)$$

For fibers with different transverse dimensions, *RWD* can be approximated from the mean *RFD* of individual fibers as

$$RWD \simeq \overline{RFD} = \frac{1}{n}\sum_{i=1}^{n}\frac{A_i}{(OP_i/4)^2} \qquad (3)$$

where the total fiber area is $(OP/4)^2$ when the fiber cross-section is assumed to be square, and n is the number of full fiber cross-sections in the image. The validity of Eq. (3) is supported by the high correlation ($R^2 > 0.88$) between the mean $(16A/(OP)^2)$ and the relative wood density calculated from Eq. (1) for the four wood samples (Fig. 12). The linear fits in Fig. 12 are similar for all samples, suggesting that the relationship between the relative wood density and $(A/(OP)^2)$ of fibers is universal. This implies that woods with similar relative densities could be comprised of fibers with a variety of fiber transverse dimensions—coarse fibers with large perimeters to fine fibers with small perimeters. Therefore, the relative wood density cannot be used to predict, for example, fiber wall cross-sectional area, or fiber coarseness (Fig. 13). The poor correlation between wood density and fiber coarseness agrees with previous observations based on the average values from the whole tree (Jang 2001; Evans et al. 1997) or wood samples at breast height (Potter et al. 2000). Fibers in

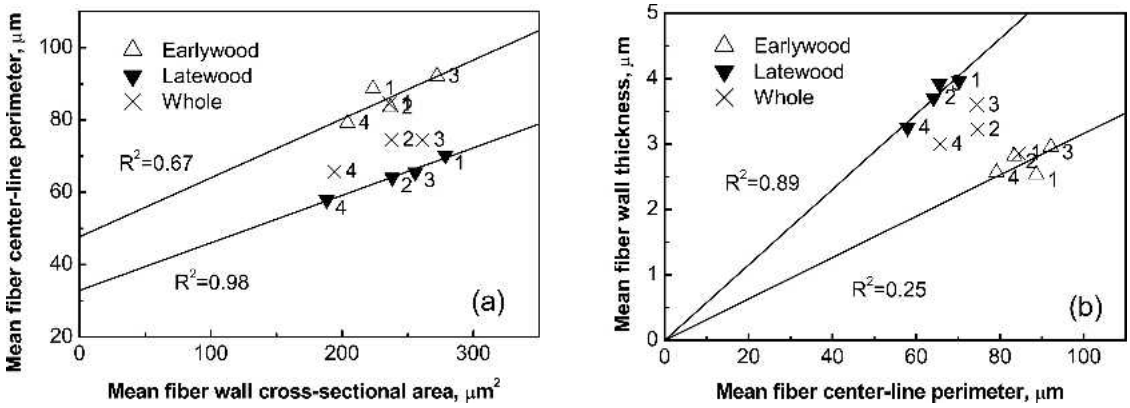

FIG. 11. Relationships among fiber transverse dimensions in earlywood, latewood and whole woods.

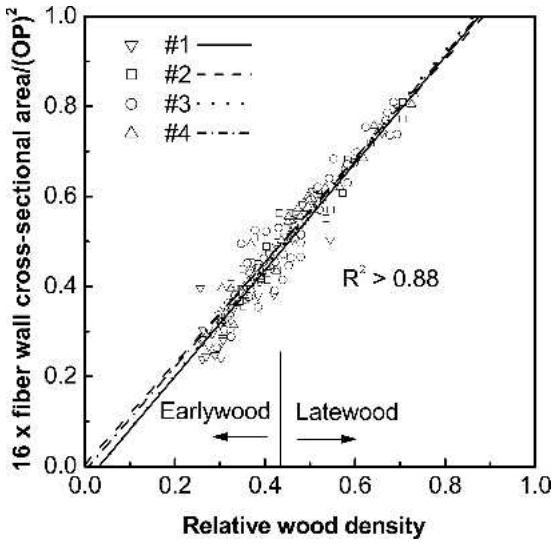

FIG. 12. Plot of $(16A/(OP)^2)$ against relative wood density for the four samples showing a high correlation.

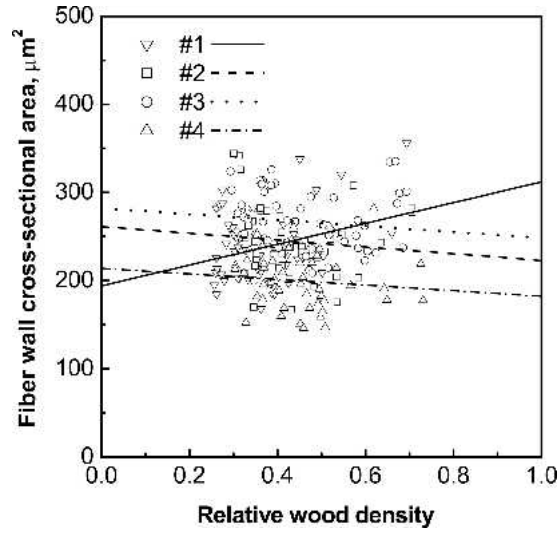

FIG. 13. Plot of fiber wall cross-sectional area against relative wood density for the four samples showing a poor correlation.

wood do have similar wall cross-sectional areas but different wall thicknesses, depending on their perimeters.

For most earlywood fibers, $T << P$, and OP can be approximated to P, the center-line perimeter. Thus, RWD can be approximated as

$$RWD \simeq \frac{1}{n}\sum_{i=1}^{n} 16\frac{T_i}{P_i} \qquad (4)$$

In other words, wood density can be approximated to (T/P) or to (T/LP) for $T << LP$, where LP is the lumen perimeter. Recall that (T/LP) is a fiber geometry factor that controls fiber collapse during papermaking (Jang and Seth 1998); fibers with small (T/LP) or a small Runkel ratio being easier to collapse. The strong correlation between shape factors, such as the Runkel ratio or Luce's shape factor, and wood density has been discussed previously (Evans et al. 1997). Thus, woods with high densities are expected to have fibers with large (T/LP) ratios, which would make them more difficult to collapse during papermaking.

SUMMARY AND CONCLUSIONS

We have demonstrated that the transverse dimensions of individual fibers in wood can be determined directly, rapidly, and accurately, without pulping it, by using confocal microscopy and image analysis. Direct measurements on wood now allow us to separately evaluate fiber transverse dimensions in early- and latewoods, and thus provide a better appreciation of their effects on pulp properties. The proportion of latewood plays a critical role in determining the heterogeneity of fiber transverse dimensions, which is important for papermaking and product properties. Relative wood density, which is calculated for each wood section, correlates poorly with fiber wall cross-sectional area, that is, fiber coarseness. However, it correlates strongly with a geometry factor, the ratio of fiber wall thickness to perimeter, on which the collapse behavior of fibers depends.

Direct optical sectioning eliminates the restriction on sample size. This technique can be applied for fiber measurements on a long wood core, or a large piece of wood. Preparation of wood samples for confocal imaging can be simple and fast for both soft- and hardwoods. An extremely high quality surface is not necessary as confocal images can be generated from below the sample surface. Fig. 14 shows a high quality cross-sectional image from a hardwood that was prepared by shaving by hand the rough surface with a razor blade. For large samples, the recent technique of using UV laser ablation in sample preparation for optical and SEM imaging could be adapted for this work (Stehr et al. 1998). This eliminates the need for mounting woods in resin, and all the subsequent sample preparation steps. Dyeing is not necessary for fluorescence imaging as wood fibers have strong auto-fluorescence, which could also be useful for a semi-quantitative assessment of lignin content distribution in wood (Moss et al. 1999). The high contrast confocal images are ready for quantitative analysis with an image analyzer (Moëll 2001).

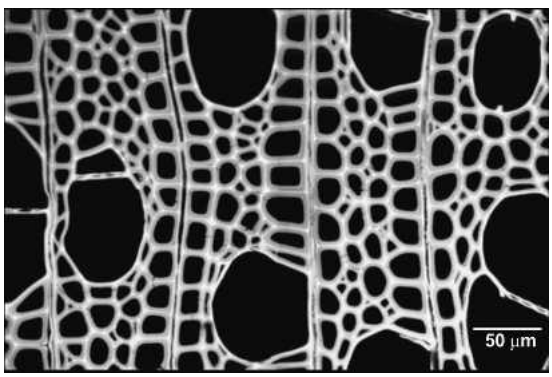

FIG. 14. Fluorescence cross-sectional image of hardwood obtained with CLSM.

Direct measurement is one of the most accurate and effective methods for characterizing fiber dimensions and its fine structures. With the advent of new technology and further development, this technique has the potential for automation, leading to a tool for rapid assessment of wood quality for papermaking.

ACKNOWLEDGMENTS

We thank John Hatton and Wai Gee for supplying the wood and pulp samples, James Drummond for his guidance on wood sample preparation, Glenn Weigel for helpful discussions, and Paul Bicho for reviewing the manuscript.

REFERENCES

ANDREWS, E. K. 1986. Impact of fiber morphology and chemical composition on the kraft process and subsequent handsheet properties. Pages 111–119 *in* Tappi Research and Development Conference Proceedings, TAPPI Press, Atlanta, GA.

CHAN, B. K., H. F. JANG, AND R. S. SETH. 1998. Measurement of fibre wall thickness by confocal microscopy and image analysis. Appita J. 51(3):229.

DONALDSON, L. A., AND M. J. F. LAUSBERG. 1998. Comparison of conventional transmitted light and confocal microscopy for measuring wood cell dimensions by image analysis. IAWA J. 19(3):321–336.

EVANS, R., G. M. DOWNES, D. N. J MENZ, AND S. L. STRINGER. 1995. Rapid measurement of variation in tracheid transverse dimensions in a radiate pine tree. Appita J. 48(2):134–138.

———, R. P. KIBBLEWHITE, AND S. L. STRINGER. 1997. Kraft pulp fibre property prediction from wood properties in eleven radiate pine clones. Appita J. 50(1):25–33.

GEE, W. Y., AND J. V. HATTON. 1991. Simple method for mass production of discrete kraft pulp samples. Tappi J. 74(2):221–222.

JANG, H. F. 2001. A theory for the transverse collapse of wood pulp fibres. Pages 193–210 *in* C. F. Baker, ed. The Science of Papermaking: Transactions of the Twelfth Fundamental Research Symposium held in Oxford, FRC, Bury, UK.

———, AND R. S. SETH. 1998. Using confocal microscopy to characterize the collapse behavior of fibers. Tappi J. 81(5):167–174.

———, A. G. ROBERTSON, AND R. S. SETH. 1991. Optical sectioning of pulp fibers using confocal scanning laser microscopy. Tappi J. (74)10:217–219.

———, ———, AND ———. 1992. Transverse dimensions of wood pulp fibres by confocal laser scanning microscopy and image analysis. J. Mater. Sci. 27:6391–6400.

KING, J. N., C. CARTWRIGHT, J. HATTON, AND A. D. YANCHUCK. 1998. The potential of improving western hemlock pulp and paper quality. I. Genetic control and interrelationships of wood and fibre traits. Can. J. For. Res. 28(6):863–870.

MOËLL, M. K., AND L. A. DONALDSON. 2001. Comparison of segmentation methods for digital image analysis of confocal microscope images to measure tracheid cell dimensions. IAWA J. 22(3):267–288.

MOSS, P., I. NYBLOM, A. SNECK, AND H-K. HYVÄRINEN. 1999. The location and quantification of lignin in kraft pulps using a confocal laser scanning microscope (CLSM) and image analysis. Pages 221–227 *in* Proc.: Microscopy as a Tool in Pulp and Paper Research and Development, Stockholm, Sweden.

POTTER, S., C. NORRIS, C. CARTWRIGHT, J. KING, W. GEE, A. HUSSEIN, M. MCRAE, S. PITTS, AND P. WATSON. 2000. Fibre and wood density assessment of western hemlock progeny, Pulp and Paper Report 1492, Paprican, Pointe-Claire, QC, Canada. 23 pp.

SCALLAN, A. M., AND H. V. GREEN. 1975. The effect of pulping upon the dimensions of wood tracheids. Wood Fiber 7(3):226–233.

SETH, R. S. 1990. Fibre quality factors in papermaking–II. The importance of fibre coarseness. Pages 143–161 *in* MRS Symposium Proceedings, Vol. 197, Materials Research Society, Pittsburgh, PA.

———, H. F. JANG, B. K. CHAN, AND C. B.WU. 1997. Transverse dimensions of wood pulp fibres and their implications for end use. Pages 473–503 *in* C.F. Baker, ed. The Fundamentals of Papermaking Materials: Transactions of the Eleventh Fundamental Research Symposium held in Cambridge, Pira International, Leatherhead, UK.

SPRENT, P. 1993. Applied nonparametric statistical methods, 2nd ed., Chapman and Hall, London. 342 pp.

STEHR, M., S. JOACHIM, AND J. INGVAR. 1998. UV laser ablation–An improved method of sample preparation for microscopy. Holzforschung 52(1):1–6.

TRAVIS, A. J., D. J. HIRST, AND A. CHESSON. 1996. Automatic classification of plant cells according to tissue type using anatomical features obtained by the distance transform, Annals Botany 78:325–331.

WILLIAMS, G. J., AND J. G. DRUMMOND. 2000. Preparation of large sections for the microscopical study of paper structure. J. Pulp Paper Sci. 26(5):183–193.

APPENDIX A

Compared to the reduction in lumen perimeter (4 ± 4%), the larger reduction in the outer perimeter (17 ± 2%) upon pulping is, in part, due to the dissolution of the lignin-rich middle lamella (Fig. 4c). Furthermore, the fiber wall being a lamellar structure, the shrinkage during delignification largely occurs radially (inwards), rather than tangentially (Fig. A). Removal of the lignin-hemicellulose matrix, therefore, mainly reduces fiber wall thickness as evidenced by the 48% shrinkage shown in Fig. 4d; its effect on perimeter is small.

APPENDIX B

The differences in chemical compositions between early- and latewood fibers are apparent in the intensity of fluorescence in wood cross-sectional images such as shown in Fig. 7 (Stehr et al. 1998). It is also known that latewood fibers produce higher yield kraft pulps, and are easier to cook to a given lignin content than the earlywood fibers (Andrews 1986). Higher yield latewood fibers would produce kraft pulp fibers with even higher coarseness and thicker walls when compared to earlywood fibers. Therefore, such yield differences would further separate wall thickness distributions of early- and latewood fibers, thus broadening the combined distribution in pulp.

Figure B1 shows the empirical distribution functions for the normalized wall thickness of fibers in wood and for pulp fibers from that wood (sample No. 2). The low K-S test shows that the distributions are different. Assuming that the earlywood fibers in wood would give a yield lower than those of the latewood fibers, and by adjusting their transverse dimensions accordingly with lower yields, we found that the empirical distribution functions for the wood and pulp fibers could be matched as shown in Fig. B2. The closest match for sample No. 2 was obtained by lowering the yield of its earlywood fibers by 15% relative to the latewood fibers.

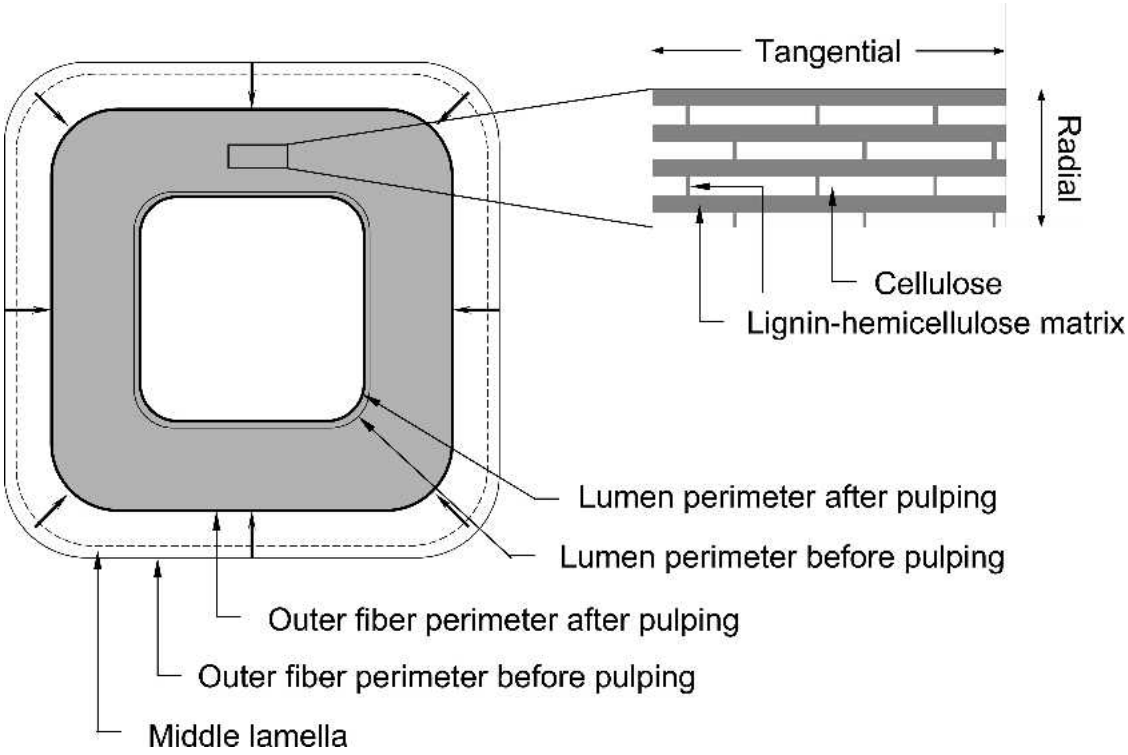

FIG. A. Schematic of radially inward shrinkage in a wood fiber wall during delignification. The inset illustrates cellulose layers (unshaded) embedded in a lignin-hemicellulose matrix (shaded) within a transverse section of the cell wall according to our data, showing more lignin-hemicellulose matrix between layers than within the layers. Therefore, the removal of the matrix during delignification leads to major wall thickness, but minor perimeter shrinkage.

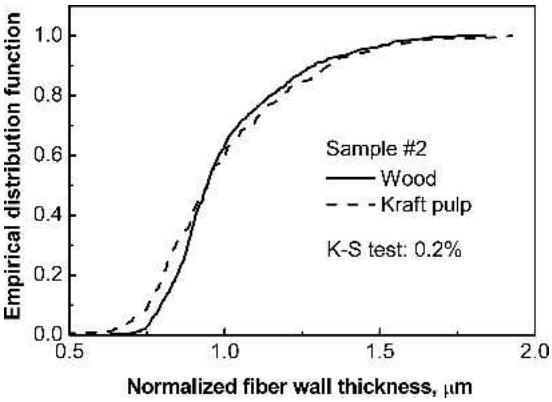

FIG. B1. Empirical distribution functions for normalized wall thickness of fibers in wood and pulp fibers obtained from that wood (sample No. 2).

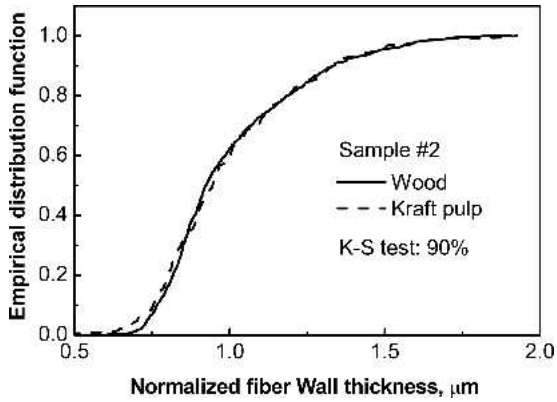

FIG. B2. Empirical distribution functions of Fig. B1 with the pulp yield of earlywood fibers lowered by 15% relative to the latewood fibers.

Such differences in yield have a small effect on *P*, but will have a large effect on *A* and *T*. However, the effect on *A* distribution is less significant than that on *T* distribution, because *A* distributions for early- and latewood fibers are nearly similar.